

Improvement of Realizations through Ranking for Oil Reservoir Performance Prediction

Stefan Zanon, Fuenglarb Zabel, and Clayton V. Deutsch

Centre for Computational Geostatistics (CCG)
Department of Civil and Environmental Engineering
University of Alberta

Abstract

There is inevitable uncertainty in the prediction of hydrocarbon recovery. This uncertainty originates from uncertainty in virtually each of the input parameters used for reservoir simulation. The variables that most significantly impact reservoir performance and hydrocarbon recovery must be identified and their uncertainty quantified. Fully sampling this space of uncertainty requires a large number of different reservoir models to be generated, all of which must undergo flow simulation. This is impractical due to the computational time required to perform every step. This paper will provide some guidance on the importance of different variables and on ways to sample uncertainty.

We create a full analytically defined space of uncertainty and illustrate how ranking can be used to sample more efficiently than MCS. The test statistic from the statistic Kolmogorov-Smirnov test is used to measure the closeness to the true distribution for Monte Carlo simulation (MCS) and ranked realizations.

Introduction

Reservoir performance prediction usually involves a two-step process: static property modelling and flow simulation. Geostatistical techniques are used to build static property models based on all available data. These models provide an estimate of the reservoir properties and a measure of the uncertainty associated with them. To perform flow simulation, a single set of static values must be chosen and the resulting flow output will be unique to that model. To account for uncertainty in static properties, multiple flow simulations are required using a suite of models that spans the space of uncertainty. Monte Carlo simulation (MCS) provides the means to build this set of models; however, this method usually requires a large number of models for accurate estimation (Ding et al., 1992). All of the models created by MCS would have to be flow simulated to provide insight into the effect this uncertainty would have on the dynamic and temporal changes in a reservoir system. This method would not be practical in most situations.

For practicality, the number of static models must be reduced while still providing a good estimate of how uncertainty is transferred to the flow simulation results. Ranking could be used to try and predict which static models will produce similar flow results (Deutsch and Srinivasan, 1996). The ranked models could then be divided into classes and a few models from each class would undergo flow simulation. The aim is to *efficiently* obtain a good estimate of how uncertainty in the static properties translates to uncertainty in reservoir performance.

Before flow simulation can be performed, the uncertainty in the static variables must be quantified. This uncertainty may be based on known errors in the sampling process, constructed

through geostatistical tools, or based on professional judgement. Great care must be taken when using the last option due to the common tendency of most people to underestimate uncertainty (Capen, 1976). Regardless of how it is assessed, uncertainty can be expressed using a distribution of possible values or a finite number of discrete levels. Distributions of uncertainty provide a spectrum of values for continuous variables. These distributions are then sampled to obtain a specific value for each variable. It is not possible to fully sample these distributions, but an approximation can be made when a large number of samples are used. Since categorical variables can only take a limited number of possible values, the full space of uncertainty is attainable due to the finite number of combinatorials. To capitalize on this, continuous variables can be limited to a few levels. The three level design is often used where the levels relate to a most likely, optimistic and pessimistic cases (Twartz et al., 1998).

Every decision in the modelling process contains some degree of uncertainty. Decisions ranging from the geological setting of the reservoir to the variance contribution for a single variogram structure are not known precisely. Trying to apply uncertainty at this level is not practical so a decision must be made as to which variables will provide the largest impact on the final flow simulation results. Sensitivity analysis will help to quantify which variables have the largest impact on flow prediction (Chewaroungroaj et al., 2000). This may require working with a simplified model to reduce flow simulation times. At the end of a study, the sensitivity of each variable can help direct efforts on how to reduce uncertainty and provide guidance for future work.

Once the most influential variables have been chosen and their uncertainty quantified, these variables must be combined to form a static model. The complexity of this step will be a combination of the complexities associated with the final model and the types of variables that contain uncertainty. For example, porosity can be defined by a single global value that is drawn from the global distribution. Alternatively, a porosity model can be constructed where every grid node has a unique distribution of uncertainty and these distributions can change depending on the modelling process used. Each static model is based on one possible combination of variables and after flow simulation this produces a unique dynamic response. To understand the uncertainty in this dynamic response, multiple static models must be constructed to span the space of uncertainty in the static variables.

There are several techniques that can be used to create the suite of static models required to sample the space of uncertainty in the static variables. Monte Carlo simulation (MCS) is a well known technique that is able to randomly sample any number of variables for use in calculating the static model. To do this, a cumulative distribution function (cdf) for each variable is calculated and independently sampled. Since there is no correlation between how the variables are sampled the number of runs must be large to ensure adequate sampling of the full (multivariate) space of uncertainty. To reduce this number, each run can be ranked while still adequately representing the space of uncertainty. For example, original oil in place (OOIP) is one such measure that could quickly be calculated for all runs and used as a ranking measure. All the runs are then binned and a few runs from each bin are selected for flow simulation. The simulation results can then be used to provide a measure of uncertainty in the dynamic response variables. Alternatively, the correlation between the dynamic variables and OOIP can be calculated and used to estimate the dynamic response for the remaining runs. This may help to provide a better measure of uncertainty in the dynamic response without performing any more flow simulations.

Displaying Uncertainty and Sensitivity

Geostatistics is “the study of phenomena that fluctuate in space.” (Olea, 1991) Due to these fluctuations, sampling this phenomenon will only provide an estimate of the different values each variable can take. This lack of information will inject uncertainty into any results derived from this information. Uncertainty in these results are expressed using a distribution of the possible values, say OOIP, where in reality there is a single unattainable value at any given time. Reporting a single value is much easier than trying to use a distribution of values in the decision making process. Displaying this uncertainty in a form that allows for easy interpretation is an important aspect of uncertainty analysis.

The histogram and cumulative distribution are two standard ways of displaying uncertainty (Deutsch et al., 2002). The histogram provides a visual representation of the shape and spread of the distribution, where each column height represents the frequency of the variable to fall in the specified range (Figure 1, left). Also seen in this figure are some statistical properties of the data: the mean, median, standard deviation, maximum and minimum values, and the upper 75th and lower 25th quartile. The cumulative distribution (Figure 1, right) displays the probability of the variable to be less than or equal to any given value. This again provides visual measure of the shape and spread of the distribution. It also provides a way to easily calculate some bounding limits on the variable. For example, an 80% probability interval is the range of values bounded by the 10th and 90th quantile.

Understanding how the output variables are sensitive to the uncertainty in the input variables is another area of interest. Identifying which variables have the largest impact on the output variables will help to determine which variables should be included in the modelling process and where to focus resources when trying to decrease uncertainty. The two primary tools for looking at sensitivity are the tornado chart and spider diagrams. The tornado chart (Figure 2, top) looks at each variable independently to determine the spread of the output variables when a lower and upper value is used. Note, all other variables are held constant at their mean or median value. The variable with the least spread is plotted on the bottom and each variable above this will have an increasing spread. Using these same results, spider diagrams (Figure 2, middle) are created by looking at the percentage of change in the input variable of interest compared to output results. The steeper the slope of the plot, the greater the impact this variable will have on the outputs. To account for the distribution of uncertainty, a quantile spider diagram (Figure 2, bottom) can be constructed where the quantile of the input variable is used instead of the percentage of change.

The Reference Data: A Synthetic Reservoir Setting

To demonstrate the transfer of uncertainty from the static variables to the dynamic flow response a synthetic petroleum reservoir example will be used. This reservoir is constructed using a 50 x 50 x 20 cell model with cell sizes of 75m in the horizontal directions and 3m in the vertical. In this model there are seven variables that contain uncertainty: well type, reservoir area, top of formation, horizontal permeability, permeability ratio, porosity, and productivity index (PI). To make the full space of uncertainty possible to obtain, each input variable is described at three levels, excluding the well type variable. These levels correspond to a pessimistic, most likely and optimistic estimate. The well type only has two possibilities, vertical or horizontal wells regardless of their application. In the vertical wells scenario, the PI is held constant since there is a much smaller degree of uncertainty when compared to the horizontal well scenario. This results in 3⁵ vertical well scenarios and 3⁶ horizontal well scenarios for a total of 972 different reservoir scenarios that underwent flow simulation.

Flow simulation can provide information on a wide range of dynamic output variables, but the focus here is on the field oil production rate (FOPR), field water production rate (FWOR), and field water injection rate (FWIR). These output variables were tracked at specific time intervals during each flow simulation run. This information was then used to calculate the net present value (NPV) of each particular reservoir scenario in terms of produced cubic metres of oil. For each time interval the NPV is calculated by:

$$NPV(i) = \frac{R_{Oil} * FOPR + C_{treat} * FWPR + C_{inject} * FWIR}{(1 + DR)^{Year}}$$

where i is the time interval, R_{oil} is the recovery rate of the oil after subtracting production costs, C_{treat} is the percentage of equivalent oil required for water treatment costs, C_{inject} is the percentage of equivalent oil required to cover water injection costs, and DR is the discount rate raised to the $year$, expressed as an integer, from the start of simulation. In this example, the R_{oil} , C_{treat} , C_{inject} , and DR were set at 0.95, 0.07, 0.05, and 0.12 respectively. The final NPV is the summation of all intervals minus the capital required for drilling the wells. The cost of drilling was approximated to be 250,000 m³ of oil for vertical wells and 375,000 m³ of oil for horizontal wells. Calculating the NPV for all scenarios yielded the full distribution of uncertainty in NPV for this reservoir. Note, the remaining variables required to build the static model and flow simulation were held constant in all scenarios.

Static Model Properties

The first variable to consider is whether horizontal or vertical well configurations will be used in the reservoir. Horizontal wells, for either production or injection, require a larger capital investment compared to the vertical alternative. The idea behind horizontal wells is that the higher oil production rates at the start of production will offset the increase in initial capital cost. The placement and number of wells changes depending on the type of well used and the size of the reservoir area. Three different reservoir areas were considered in this example and are referred to as small (sml), middle (mid), and big. These reservoir areas correspond to 53.3%, 73.2%, and 86.5% of the total model area, respectively. The largest area used 7/4 (producers/injectors) and 9/4 for the horizontal and vertical scenarios, respectively. The middle and small areas used 6/3 and 3/2 for the horizontal scenarios and 7/4 and 5/4 for the vertical scenarios, respectively. The well placement for each well type and area can be seen in (Figure 3) where the reservoir area is in grey, production wells are in black, and injector wells are in white. The configuration of the wells could be optimized to provide better results, but this is beyond the scope of this study.

The top of the reservoir was stochastically modelled using input data at the centre and edges of the area. In the middle of the area, 8 data points were used to act like exploratory wells along with 8 more data points at the edge of the area to control the degree of curvature in the surface. The surfaces were created using SGSIM (Deutsch and Journel, 1998) where all the parameters were held the same except the input data and mean. As a result, all three surfaces have the same basic structure. To distinguish between them, each surface is referred to by its respective mean. An approximately flat surface was created by using centre and edge points that were at similar depths with a mean depth of 2,994 m. To produce a small curve, the edge points were decreased for a new mean of 2,999 m. The curvature was further increased by lowering the edge points even more resulting in a mean of 3,005 m. When comparing these three surfaces, the global variances of 1.32, 4.34, and 7.86, respectively, can be used to help quantify the degree of

curvature. The surfaces represent the top of the formation with a depth range between 2,990 m and 3,010m in depth (Figure 4).

A single horizontal permeability value was used for all cells in both horizontal directions. The horizontal permeability levels were set at 500, 1000, and 1500 mD. To obtain the vertical permeability, a permeability ratio was used to link the vertical to the horizontal permeability. The levels for this ratio were 0.4, 0.5, and 0.6. To calculate the vertical permeability, the current horizontal permeability was multiplied by one of the above ratios.

The final two static variables are the porosity and productivity index. The levels for porosity were set at 0.10, 0.15, or 0.20. The production index (PI) is a measure of the effective length and damage ratio of a well. For horizontal wells it is difficult to simulate these conditions in simple flow models' as used in this example. To cover the different possibilities, the PI was set at 8, 20, and 50 m³/day/kgf/cm² depending on the horizontal well scenario. These considerations were ignored for the vertical well scenarios and a constant PI of 4 m³/day/kgf/cm² was used for all runs. The values used for each variable and level are summarized in Table 1.

	Reservoir Area	Production Index	Alter Top Surface	Perm. Ratio (Vertical)	Perm. XY	Porosity
Vertical Wells	Sml	4	2994	0.4	500	0.10
	Mid		2999	0.5	1000	0.15
	Big		3005	0.6	1500	0.20
Horizontal Wells	Sml	8	2994	0.4	500	0.10
	Mid	20	2999	0.5	1000	0.15
	Big	50	3005	0.6	1500	0.20

Table 1 Different values used for each variable and level in the example.

In this example, the chosen value for each variable can be directly used in flow simulation and intermediate steps are not required to combine the variables into a static model, such as kriging or simulation.

Flow Simulation

This reservoir is situated at a depth around 3000 m, as seen by the top surface (Figure 4), and has a thickness of 60 m. The initial reservoir pressure is 315 barsa at a reference depth of 3015 m. The oil/water contact is always below the base of the reservoir at a depth of 3080 m, but the larger the top surface curvature, the closer this contact is to the base. The number of wells and their locations (Figure 3) change depending on the reservoir area and type of wells used. Well control parameters changed depending on the well type, as summarized in Table 2. All the other required parameters needed to perform the flow simulation were based on a medium oil scenario in an Albertan basin.

Orientation	Well Type	Control	Perforation Range (layer)	Minimum BHP (barsa)	Maximum BHP (barsa)	Maximum Rate (m ³)
Vertical Wells	Producer	BHP	1 to 10	125		1500
	Injector	BHP	1 to 20		360	2000
Horizontal Wells	Producer	BHP	3	125		2000
	Injector	BHP	15		360	3000

Table 2 Well control parameters used in flow simulation.

The production life of this reservoir was estimated to be 20 years and flow simulation was performed to track the dynamic reservoir response over this interval. Specific dates were used to output the required dynamic variables so that the time steps would be the same for all runs. These dates were chosen as small as a single day at the start of flow simulation and increased to a maximum of six months in the later years.

Flow simulations were performed using ECLIPSE 100 (Schlumberger, 2002) on a 2.27 GHz IBM compatible desktop computer with 1.0 GB of RAM. To help automate the simulation process, bash scripting was used to create and run all the models and to post process subsequent results. A program was created to calculate the NPV for each scenario based on the output from ECLIPSE and the number and type of wells used for that run. These results were then used to assess the uncertainty after flow simulation. The time requirement for each flow simulation ranged between about 5 to 7 minutes, resulting in several days of computer processing to fully sample the space of uncertainty. As the model complexity increases and more input variables are used, the computation requirements will increase, making the full space of uncertainty impractical to sample.

Uncertainty Assessment

In this example the full space of uncertainty was accessible by flow simulating all 972 different possible combinations of the seven input variables, (Figure 5, left). For any subset of this space the resulting uncertainty can be compared against this distribution to provide a measure for the error in the NPV uncertainty. These results also provide the true relationship between NPV and OOIP, (Figure 5, right). The two variables have a good relationship with a rank correlation of 0.775, indicating that the OOIP should work well as a ranking variable.

For most reservoirs the full space of uncertainty would not be calculated. Only a limited number of runs would undergo flow simulation, and the number of runs and how they are chosen will directly impact the estimated distribution of uncertainty. To calculate the error in the distribution of uncertainty the subset cdf was compared with the full space cdf using 99 points along the cdfs ranging from the 0.01 quantile to the 0.99 quantile. The cumulative absolute error between the cdfs provides an indication of how well that subset estimated the distribution of uncertainty.

For this example the MCS and ranked MCS methods were used to choose the runs based on a specific number in a subset. The following numbers of runs per subset were considered: 10, 20, 30, 40, 50, 75, 100, 150, 200, 300, 400, 500, 700, and 900. The only restriction placed on these methods when choosing the runs was that each run must be unique. Since there is no accounting for how well the space of uncertainty is sampled, for a given number of runs 51 different subsets

were calculated. All these results were then plotted together to demonstrate how well MCS and ranked MCS perform as the number of runs in each subset increases (see Figure 6).

In general, both the MCS and ranked MCS demonstrate two things as the number of runs in a subset increases: the absolute error will decrease and the variability between subsets decreases. It is also observed that for a given number of runs the variability is always smaller when ranking is used. These statements are confirmed by comparing the statistics for each specified number of runs and between the MCS and ranked MCS methods, Table 3 and Table 4, respectively. From these tables it is seen that the average value and standard deviation continuously decrease as the number of runs increase, this applies to the levels not shown. When comparing the statistics between the two methods for a given number of runs, the mean and standard deviation are always smaller for the ranked MCS results.

MCS									
	10	20	50	100	200	300	500	700	900
Max	1724.6	1380.1	684.1	584.0	342.1	341.3	156.1	102.8	58.5
Min	161.6	233.8	125.0	126.6	78.8	62.7	39.7	25.0	11.7
Mean	736.0	585.1	352.9	236.4	171.2	138.4	88.1	55.0	26.3
St. Dev.	356.8	224.1	119.3	91.2	55.2	64.3	30.7	19.2	10.2

Table 3 The statistics for a given number of runs using MCS.

Ranked MCS									
	10	20	50	100	200	300	500	700	900
Max	1109.9	775.6	424.9	368.3	185.8	183.6	112.3	77.7	40.5
Min	263.8	202.0	127.8	91.5	73.0	54.6	37.7	25.4	10.8
Mean	560.1	439.0	250.9	169.1	125.5	99.3	60.9	43.7	21.7
St. Dev.	176.6	129.6	63.7	50.7	23.7	27.5	16.0	12.6	7.2

Table 4 The statistics for a given number of runs using ranked MCS.

Measuring Reservoir Performance Prediction

The MCS and ranked MCS results in the previous section are interesting; however, we can take this one step further and see how well we can infer the reference uncertainty distribution due to (1) the number of realizations and (2) the sampling methodology.

Let's consider the number of realizations drawn to determine an uncertainty distribution for NPV. MCS was performed to randomly sample the 972 runs with no replacement, for a variety of subsets of realizations and for 1000 times for each subset. While the tables above summarize some of these results, Figure 7 shows the uncertainty in the NPV distribution when different sets of L realizations are drawn (in the figure, $L=10, 30, 60, 100, 200,$ and 500 realizations). The thick line in each plot represents the reference cdf of NPV obtained from the 972 runs. It can be seen that the larger the number of MCS realizations is, the more the sampling cdf approaches the true cdf distribution.

A Kolmogorov-Smirnov test (Harnett, D.L., 1982) was performed to measure the closeness between the sampling cdf and the true cdf. This test statistic is easy to compute. It was done by

calculating the maximum value of absolute difference (D value) between the true cdf and the sampling cdf of 9 quantiles (0.1, 0.2, ..., 0.9) for each realization as follows.

$$D = \text{Max}_i | F_i - S_i |$$

where F_i = true cdf and S_i = sampling cdf.

Table 5 gives some critical values of D for various probability values and Figure 8 gives the full cdf of $D\sqrt{n}$ where n is the sample size. Figure 9 shows the relationship between critical values of D and the sample sizes at different levels of significance. Figure 10 shows the constant values of $D\sqrt{n}$ vs \sqrt{n} for different levels of significance.

Since sampling NPV was drawn for 1000 times for each number of realizations; therefore, distribution of D value for each realization can be obtained. Figure 11 shows the P10, P50, and P90 in the calculated D values for each realization, while Figure 12 shows the corresponding mean and standard deviation of D values. It can be seen that the higher the number of sampling data, the lower the error in the distribution of uncertainty as it approaches the full space of uncertainty. It should be noted that this MCS is drawn from a finite population. As a result, we find that uncertainty in the D value is reduced more quickly as the number of realizations (> 200) approaching the population size (972). As a result, the slope of the log-log plot of D value vs number of realizations deviates from 0.5 to an average of 0.58.

To evaluate the methodology, let's look now at the ranked MCS sampling approach. For this task, the original oil in place (OOIP) was chosen as a ranking measure since it is quick to calculate and has a good correlation with NPV of 0.755 (see Figure 5). Specifically, the following methodology was undertaken:

1. Perform MCS to draw larger amount of realizations then rank realizations. For example, draw 100 MCS realizations for 20 rank realizations.
2. Sort corresponding OOIP in ascending order. Cumulative distribution function of OOIP for the drawn MCS realizations was then plotted and shown in Figure 13.
3. Select rank realizations that are equally spaced from MCS realizations to cover the space of uncertainty.

The equally spaced quantiles to be selected can be calculated as follows.

$$P_i = \frac{i - 0.5}{L}$$

where P_i = selected quantiles, $i = 1, 2, \dots, L$ rank realizations, and L = number of realizations

4. Corresponding flow response of the selected rank measures can be obtained from flow simulation. Figure 14 shows the comparison between the cdf of selected NPV and true cdf.
5. The maximum absolute difference (D value) between the true cdf and the rank cdf of 9 quantiles was calculated in a similar manner as mentioned above for MCS.

The comparison of D value distribution between MCS and ranked MCS is shown in Figure 15 for P10, P50, and P90 and in Figure 16 for mean and standard deviation. A similar trend to the MCS

is observed with an average of slope of 0.54 for the log-log plot of D value and number of realizations. These plots clearly show lower distribution of D values obtained from ranking.

Figure 17 shows the comparison of mean D values for MCS and ranked MCS with K-S critical D values at different significant levels. A higher level of significant with the value of 0.95 is observed for the ranked MCS. Percent improvement was calculated to illustrate how ranking can improve reservoir management by reducing the number of realizations to be processed but still represent the same uncertainty as MCS (see Figure 18). It shows an increasing percent of improvement of ranking over MCS with more uncertainty.

Sensitivity Assessment

Working with the full space of uncertainty ensures that the desired runs for sensitivity analysis have been performed. The sensitivity was looked at for the horizontal and vertical well scenarios separately with 6 variables for the horizontal wells and 5 variables for the vertical wells. The sensitivity for each variable is described by looking at each level of the variable with all other variables at their base value. The point of intersection of all variable per well case is the value of NPV when all variables are at their base value. This analysis requires a total of 24 specific runs to describe the sensitivity using spidergrams, (Figure 19) and tornado charts, (Figure 20), for the true horizontal and vertical well scenarios, left and right respectively.

When using the MCS and the ranked MCS methods to determine the subsets, no consideration is placed on using the runs required for sensitivity analysis. To overcome this problem a new way of calculating the sensitivity is proposed. For each variable, an average NPV is calculated using all the results that contain the level of interest, ignoring the other variables. These averages are then used to create the spidergrams, (Figure 21), and tornado charts, (Figure 22), for the horizontal and vertical well scenarios, left and right respectively. Note that the centre point for each variable is different due to how the data is separated. These results are very similar to the true sensitivity figures. The magnitude of the sensitivity for each variable, as seen by the spread in the tornado charts and the slope of the spidergram, is very similar for both results. The tornado charts also provide the order from the most sensitive, top, variable to the least sensitive, bottom, variable. The order of these variables is the same for the average and true results with the exception of the two least sensitive variables for the horizontal wells.

Conclusions

A true space of uncertainty was constructed for a realistic petroleum problem. The true distribution of NPV was established and it was sampled by MCS and through targeted ranked realizations. For a given number of realizations, the ranking gets significantly closer to the true distribution. The use of a quantitative measure such as Kolmogorov-Smirnov's D statistic further confirms that the ranked MCS approach was more efficient than the MCS approach.

In practice, uncertainty assessment in reservoir modelling will be performed using only a limited number of flow simulations due to time limitations. In addition to the improved results through realizations ranking, we also showed how sensitivity is possible with only a limited number of runs. The averaging method provides a way to perform sensitivity analysis on these limited runs. In this example the variables that provide the most impact in decreasing order are the reservoir area, the production index (horizontal wells only), the porosity, and the horizontal permeability. The top surface and vertical permeability had almost no impact on the output uncertainty. Understanding what the model is sensitive to can help to direct how future data collection is

performed. Reducing the uncertainty in the most sensitive variable will provide the greatest reduction in uncertainty.

Acknowledgements

We would like to acknowledge the industry sponsors of the Centre for Computational Geostatistics at the University of Alberta for supporting this research. The support of the National Science and Engineering Research Council of Canada (NSERC) is also acknowledged.

References

- Capen, E. C., *The Difficulty of Assessing Uncertainty*, Journal of Petroleum Technology, August, 1976, p. 846-850.
- Chewaroungroj, J., Varela, O. J., and Lake, L. W., *An Evaluation of Procedures to Estimate Uncertainty in Hydrocarbon Recovery Predictions*, Society of Petroleum Engineers, 59449, 2000.
- Damsleth, E., and Hage, A., *Maximum Information at Minimum Cost: A North Sea Field Development Study with an Experimental Design*, Journal of Petroleum Technology, 1992, p. 1350-1356.
- Deutsch, C. V. and Srinivasan, S., *Improved Reservoir Management Through Ranking Stochastic Reservoir Models*, Society of Petroleum Engineers, 35411, 1996.
- Deutsch, C. V. and Journel, A. G., *GSLIB: Geostatistical Software Library and User's Guide*, 2nd Edition, Oxford University Press, 1998.
- Deutsch, C. V., Monteiro, M., Zanon, S., and Leuangthong, O., *Procedures and Guidelines for Assessing and Reporting Uncertainty in Geostatistical Reservoir Models*, Centre for Computational Geostatistics, Report 4, 2002.
- Ding, L., Mehra, R. K., and Donnelly, J. K., *Stochastic Modeling in Reservoir Simulation*, Society of Petroleum Engineers, 18431, 1992.
- ECLIPSE Reference Manual 2002A*, Schlumberger, 2002.
- Harnett, D.L., *Statistical Methods*, 3rd Edition, Addison-Wesley Publishing Company, 1982.
- Olea, R. A., *Geostatistical Glossary and Multilingual*, Oxford University Press, 1991.
- Twartz, S. K., Gorjy, F., and Milne, I. G., *A Multiple Realisation Approach to Managing Uncertainty in the North Rankin Gas Condensate Field, Western Australia*, Society of Petroleum Engineers, 50078, 1998.

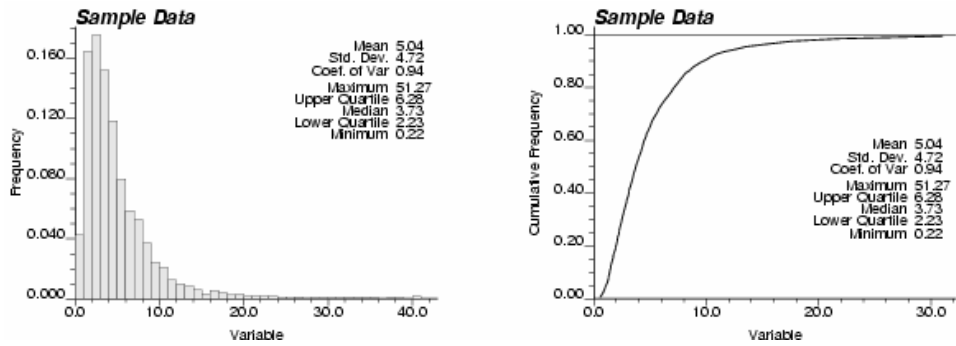


Figure 1 Histogram and cumulative distribution of sample data to show how to display uncertainty.

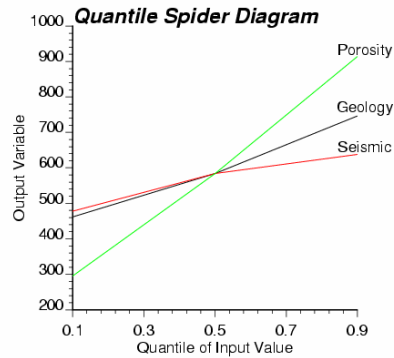
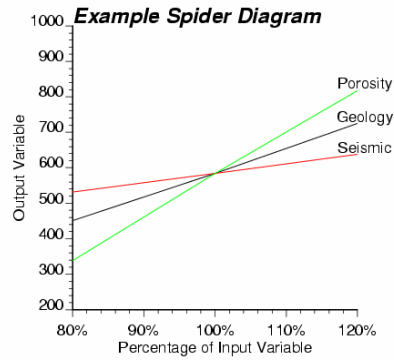
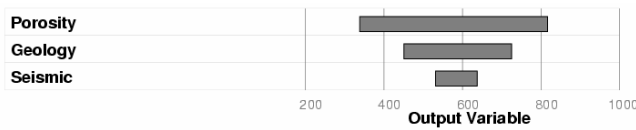


Figure 2 An example of a tornado chart (top) and spider diagrams (middle) and quantile spider diagrams (bottom).

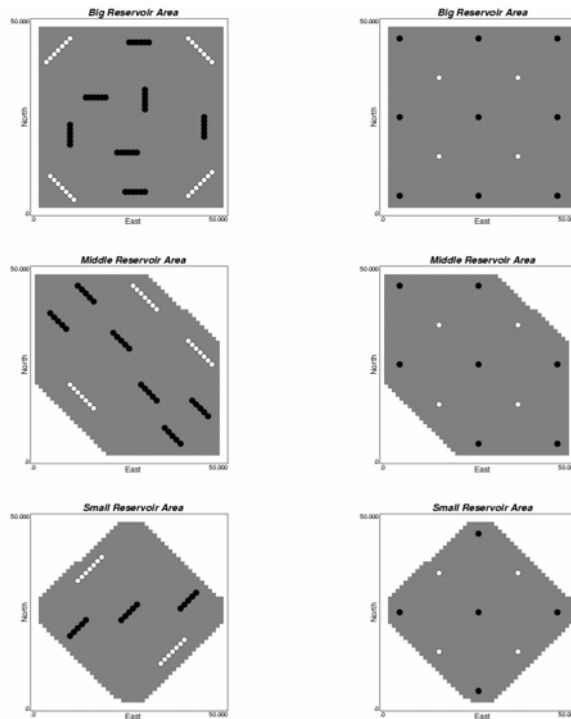


Figure 3 The location of the horizontal (left) and vertical (right) wells for the three possible reservoir areas. Production wells are seen in black and injection wells are seen in white.

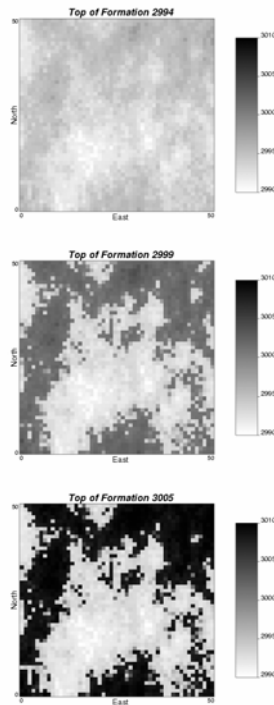


Figure 4 Plots of the three top of formation scenarios used in the example.

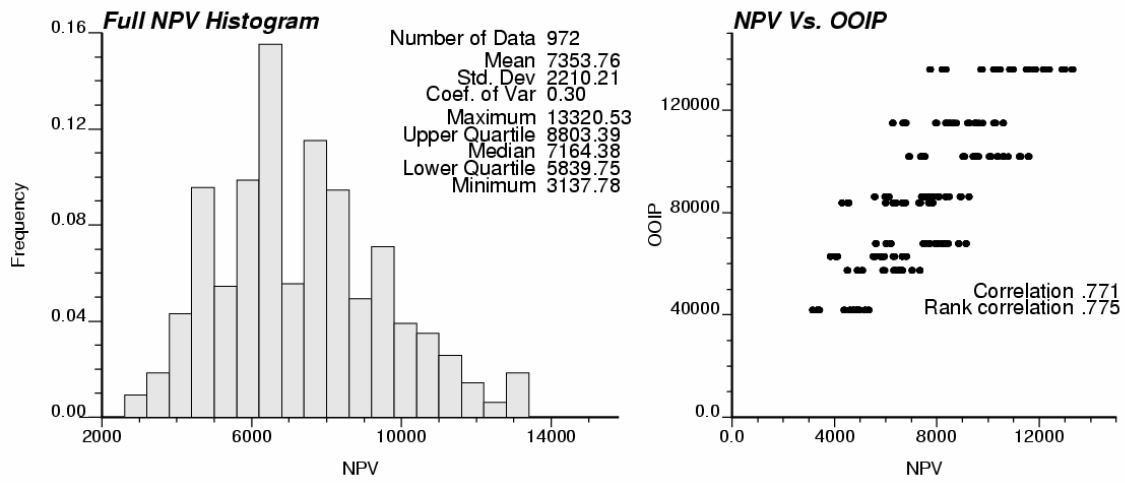


Figure 5 True histogram of NPV uncertainty and the scatter plot between NPV and OOIP.

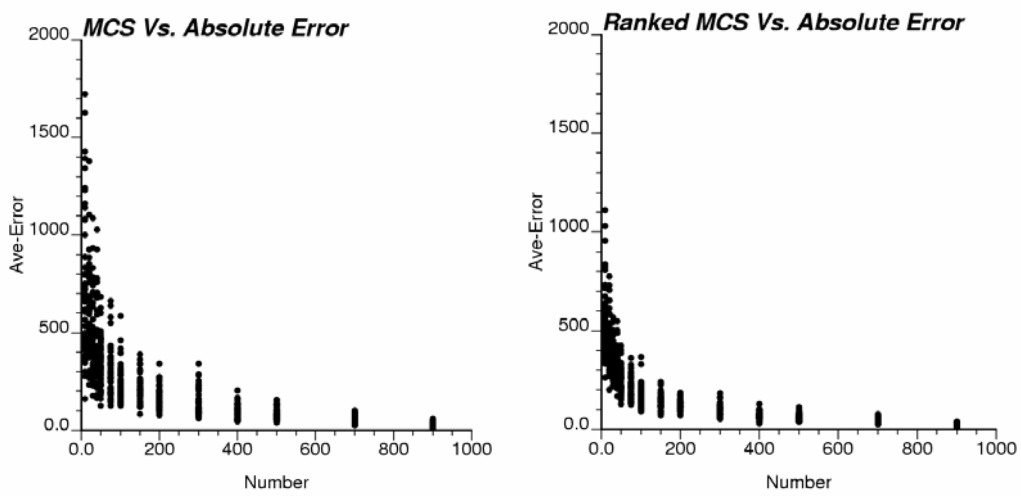


Figure 6 A scatter plot showing the average error in the MCS cdfs (left) and the ranked MCS cdfs (right) for different number of runs.

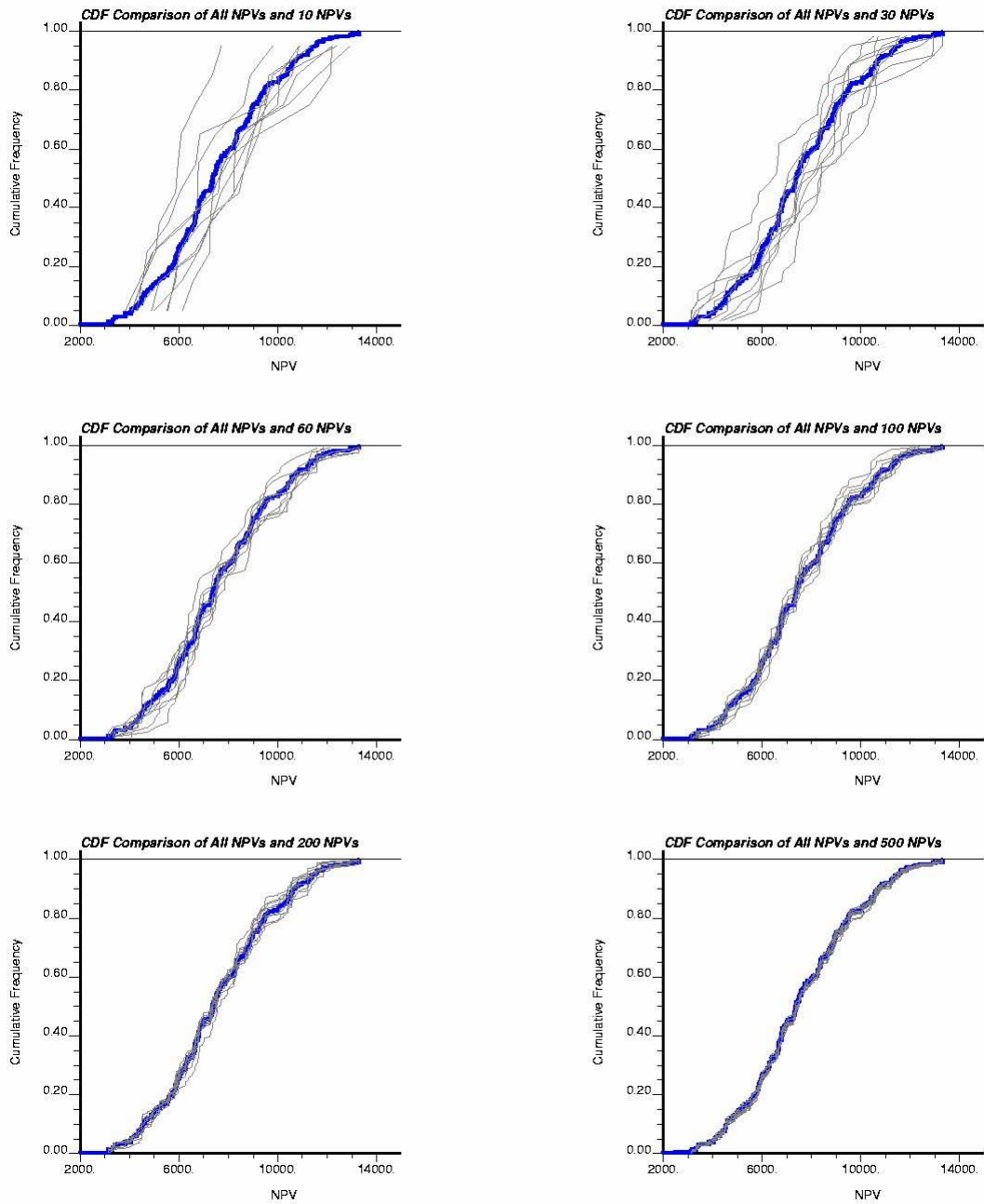


Figure 7 Comparison between true CDF of NPV and sampling CDF of NPV for different realizations.

Sample size (n)	Level of significance for D where $D = \text{maximum } F_i - S_i $				
	0.20	0.15	0.10	0.05	0.01
1	0.900	0.925	0.950	0.975	0.995
2	0.684	0.726	0.776	0.842	0.929
3	0.565	0.597	0.642	0.708	0.828
.
.
.
25	0.21	0.22	0.24	0.27	0.32
30	0.19	0.20	0.22	0.24	0.29
35	0.18	0.19	0.21	0.23	0.27
Over 35	$.07/\sqrt{n}$	$1.14/\sqrt{n}$	$1.22/\sqrt{n}$	$1.36/\sqrt{n}$	$1.63/\sqrt{n}$

Table 5 Critical Values of D in the Kolmogorov-Smirnov

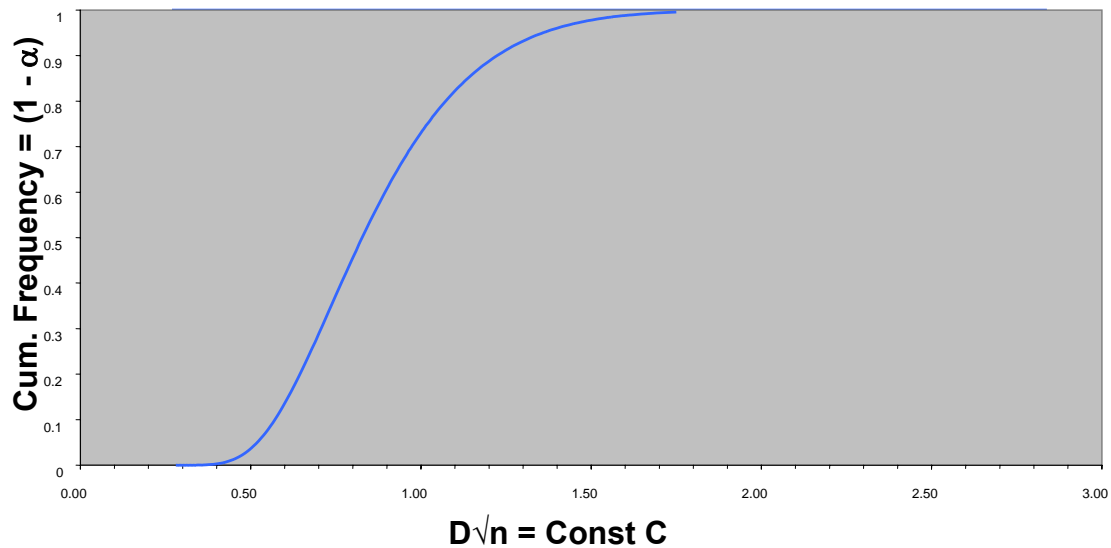


Figure 8 CDF plot of $D\sqrt{n}$, where α is level of significance and constant C values are 1.07, 1.14, 1.22, 1.36, and 1.63 for α of 0.20, 0.15, 0.10, 0.05, and 0.01, respectively.

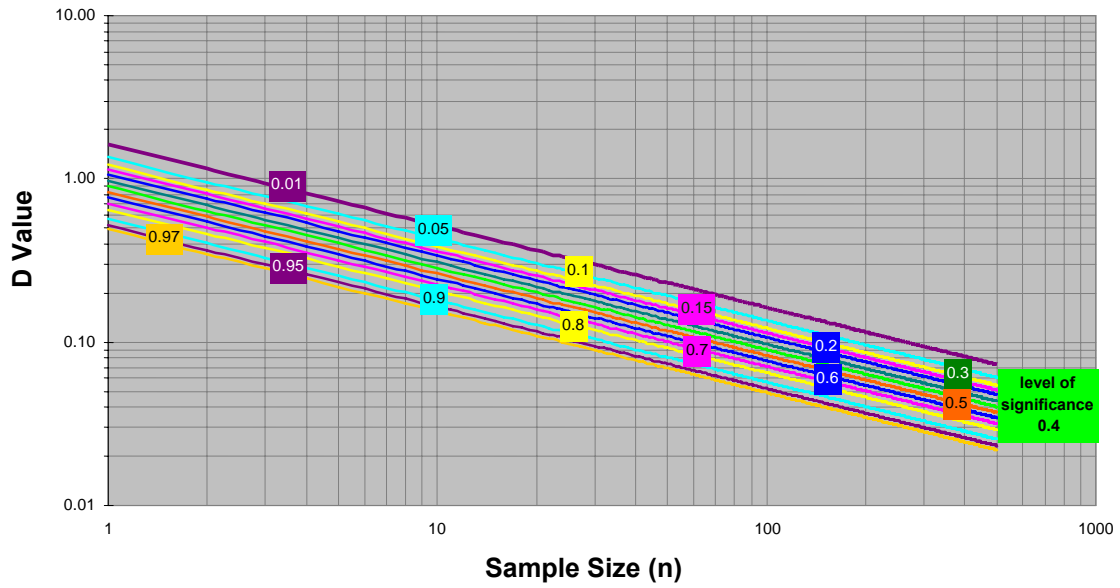


Figure 9 Kolmogorov-Smirnov critical values of D vs sample sizes at different levels of significance.

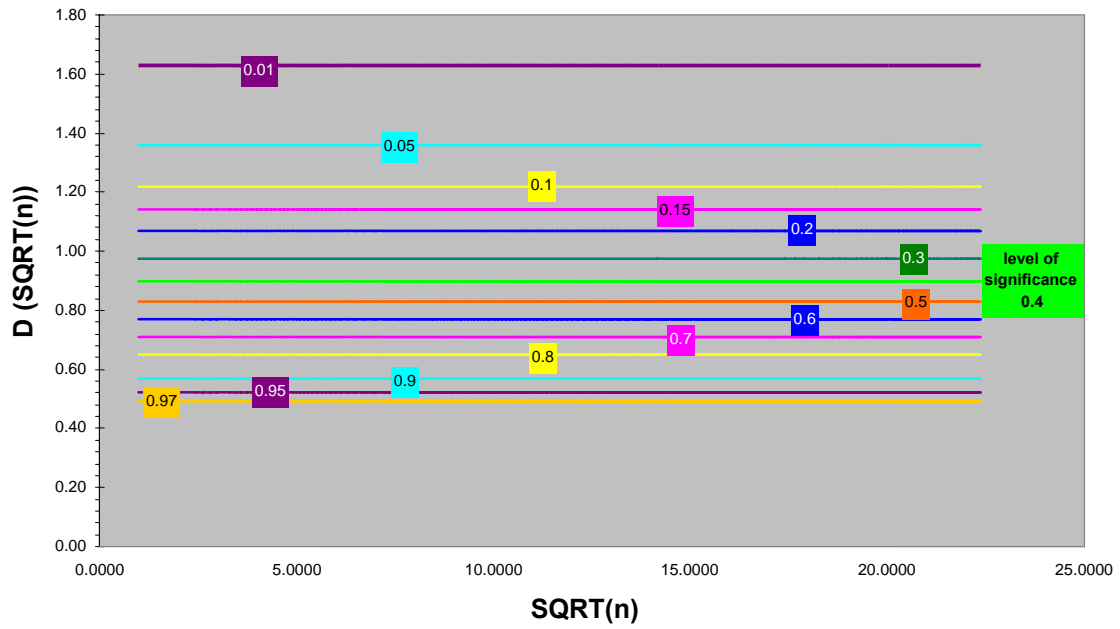


Figure 10 Constant values of $D\sqrt{n}$ vs \sqrt{n} for different levels of significance.

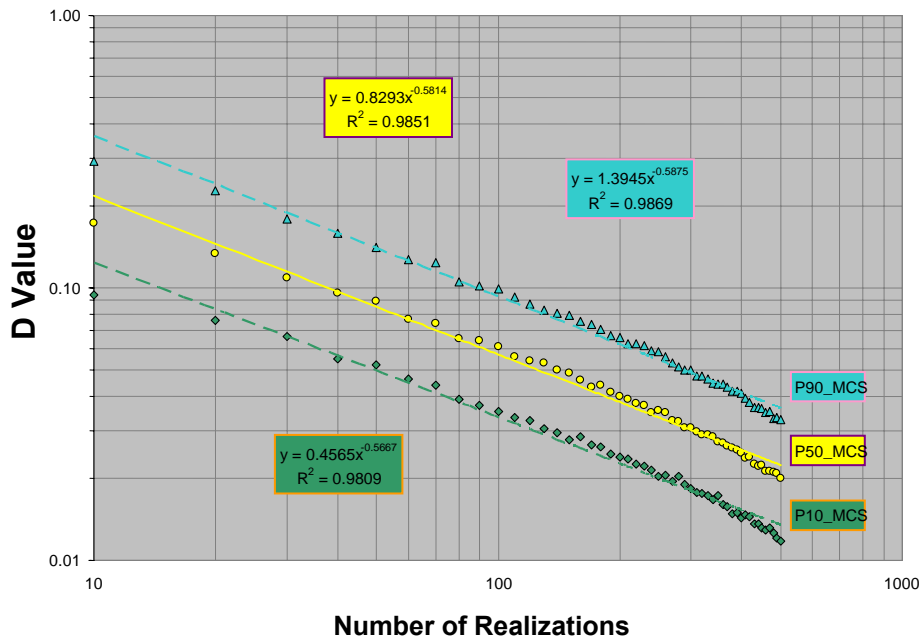


Figure 11 D value distribution (P10, P50, and P90) for MCS.

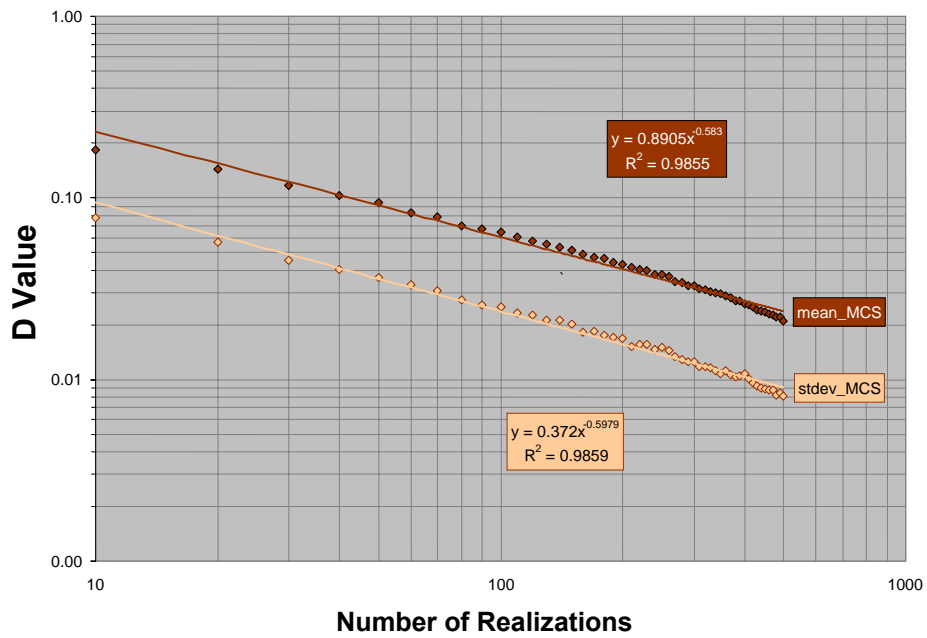


Figure 12 D Value Distribution (mean and standard deviation) for MCS.

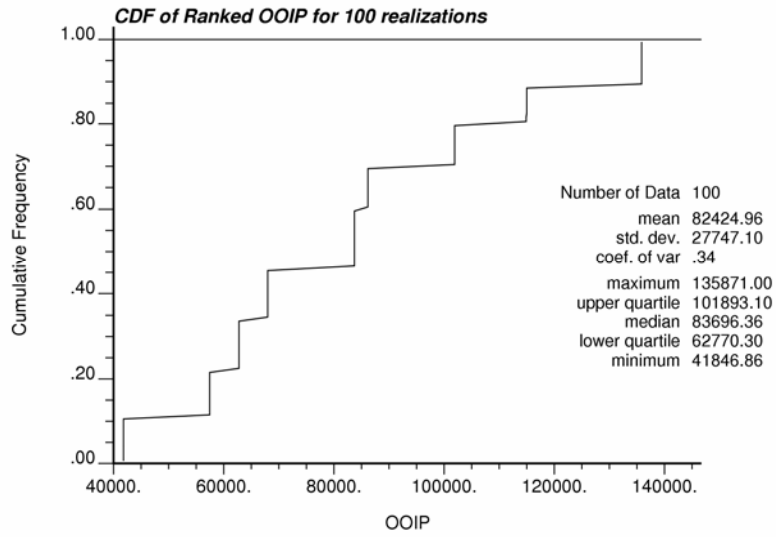


Figure 13 CDF of ranked OOIP for 100 realizations.

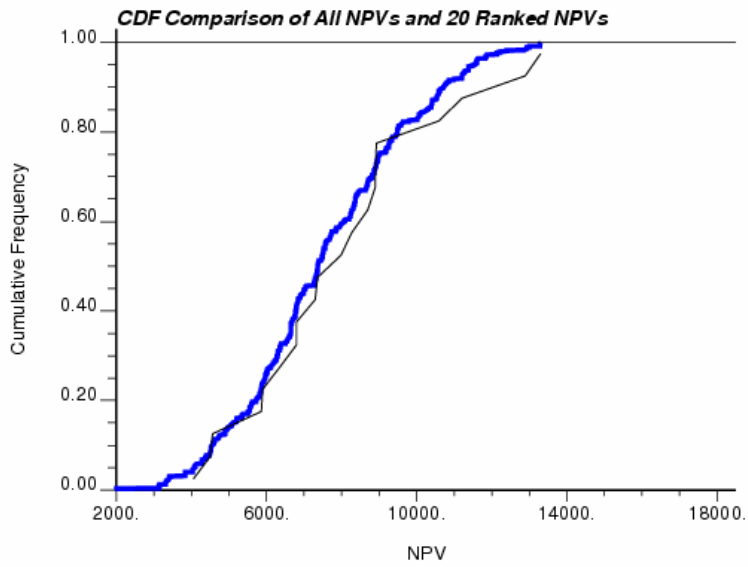


Figure 14 Comparison between CDF of selected 20 ranked NPVs and that of true distribution.

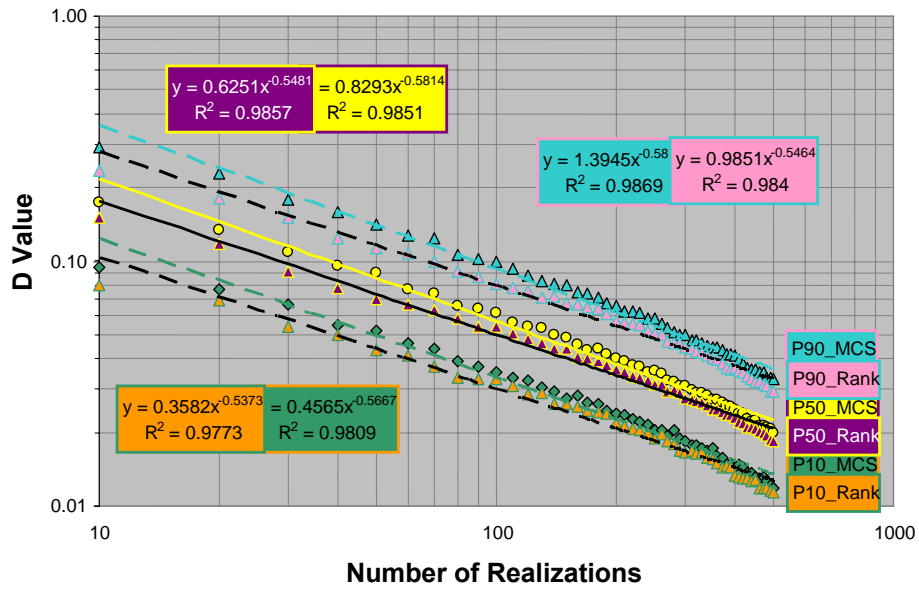


Figure 15 Comparison of D value distribution between MCS and ranked MCS.

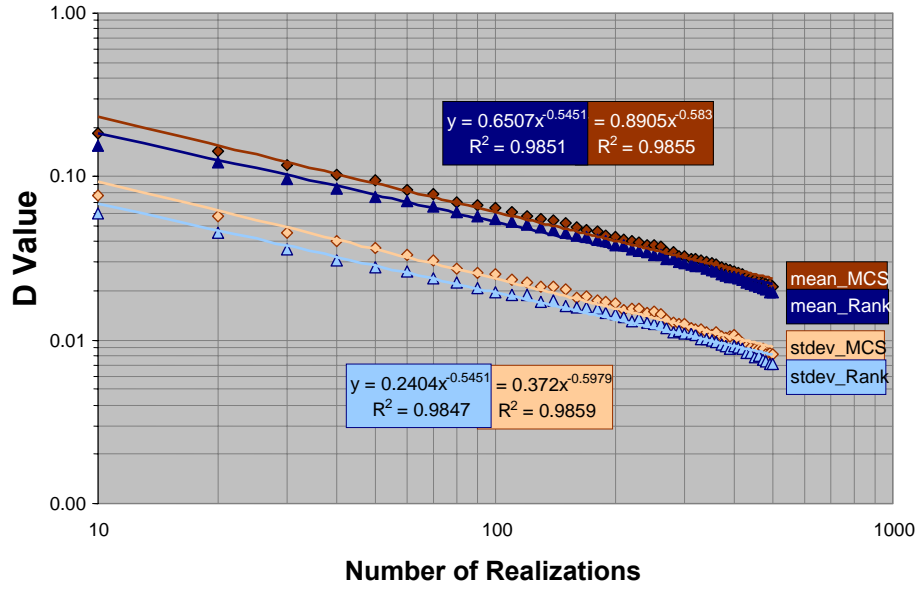


Figure 16 Comparison of D value distribution between MCS and ranked MCS.

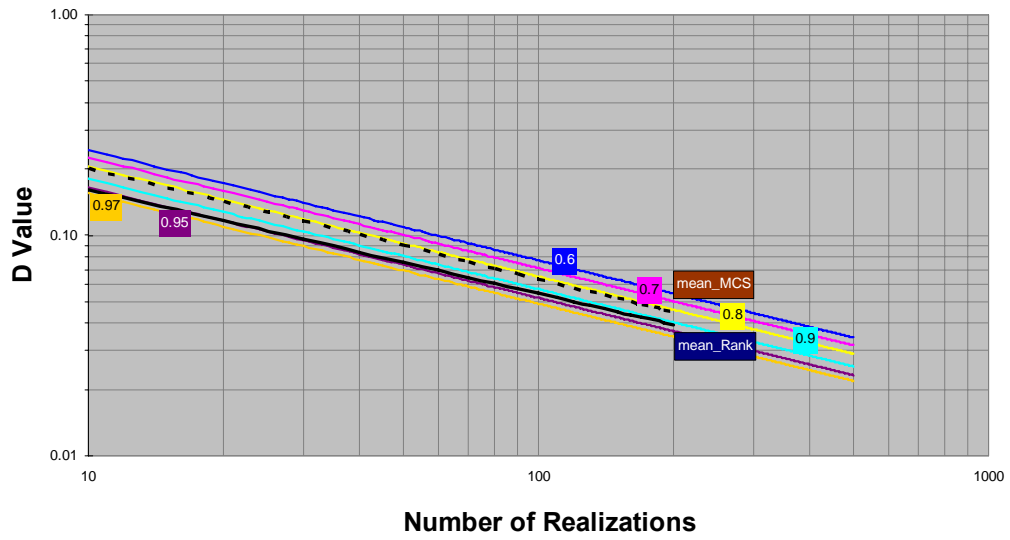


Figure 17 Comparison between K-S D values and D values from MCS and ranked MCS.

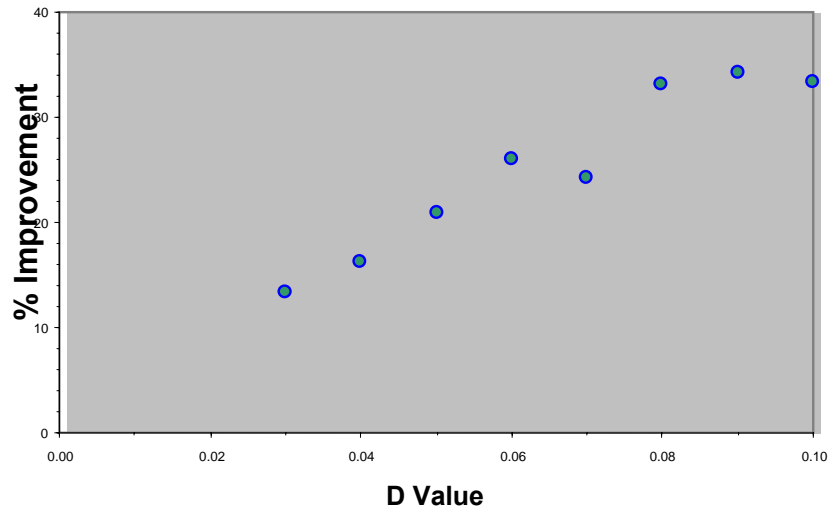


Figure 18 Improvement of Ranking over MCS by Using OOIP as a Ranking Measure with a High Correlation Coefficient of 0.755 with NPV.

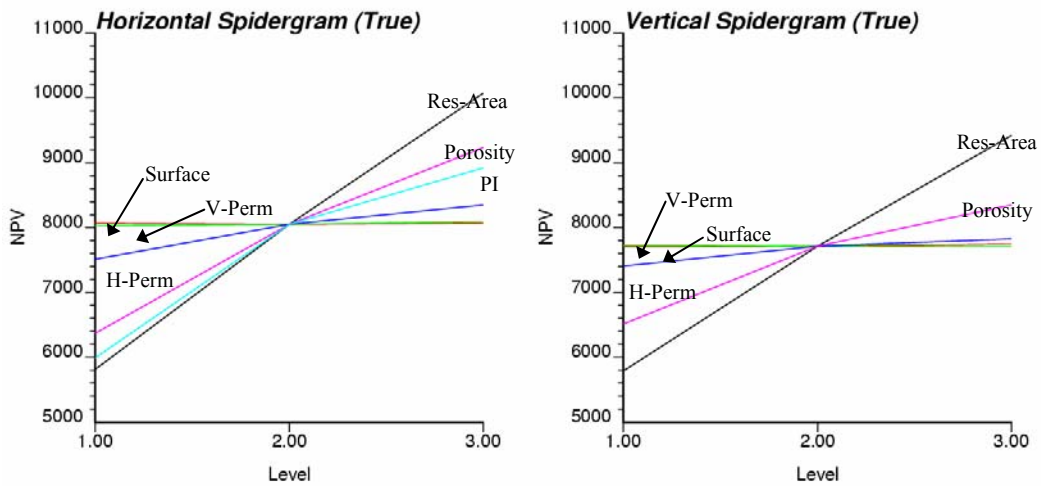


Figure 19 The spidergrams for the true horizontal and vertical well scenarios.

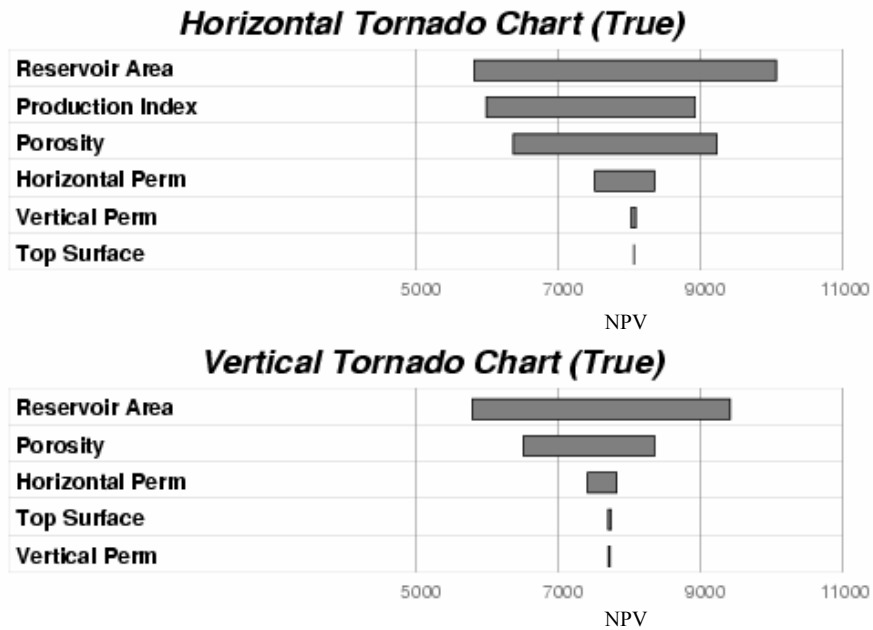


Figure 20 The tornado charts for the true horizontal and vertical well scenarios.

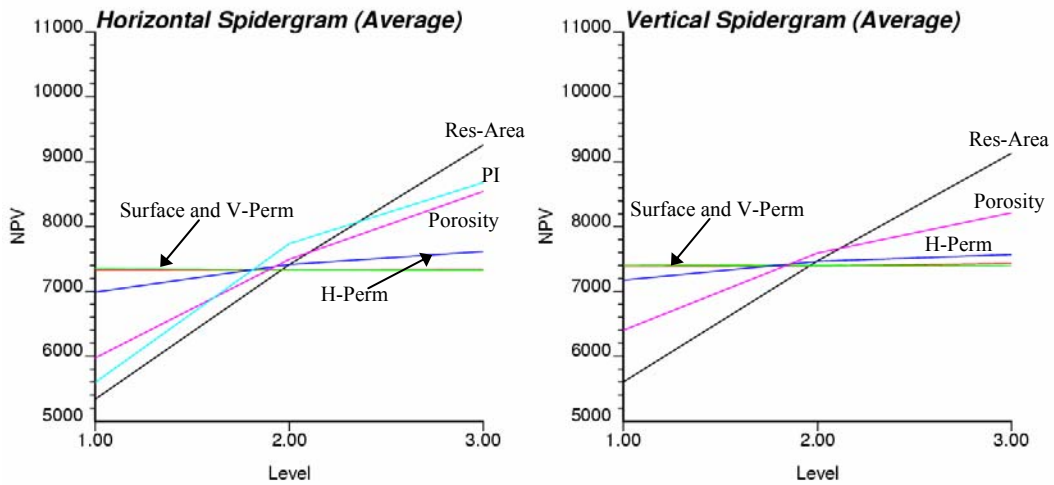


Figure 21 The spidergrams for the averaged horizontal and vertical well scenarios.

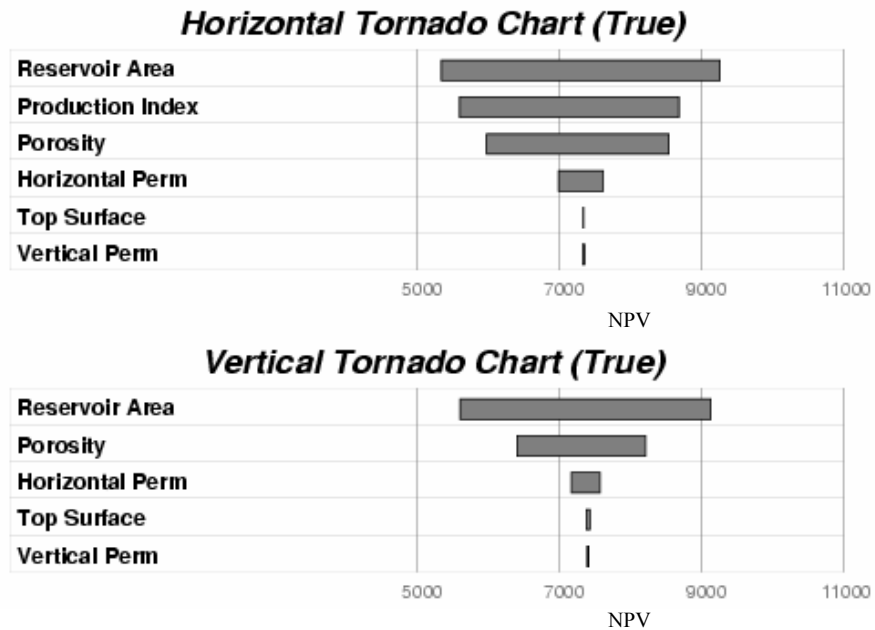


Figure 22 The tornado charts for the averaged horizontal and vertical well scenarios.